Research Square

Preprints are preliminary reports that have not undergone peer review.
They should not be considered conclusive, used to inform clinical practice,
or referenced by the media as validated information.

In Vitro and In Silico Evaluation of the Efficacy and Safety of a Ghanaian Herbal Medicine for the Treatment of Onchocerciasis and African Trypanosomiasis

Barbara Zenabu Anibea
bzanibea@st.ug.edu.gh
University of Ghana

Eric Coffie
ericcoffie@ug.edu.gh
University of Ghana

Daniel Moscoh Ayine-Tora
dmayine-tora@ug.edu.gh
University of Ghana

Theresa Manful Gwira
tmgwira@ug.edu.gh
University of Ghana

Dorcas Osei-Safo
dosei-safo@ug.edu.gh
University of Ghana

Research Article

Keywords: Herbal medicine, safety, Xylopia aethiopica, Bambusa vulgaris, Onchocerciasis, Animal Trypanosomiasis, phthalate

DOI: https://doi.org/

License: This work is licensed under a Creative Commons Attribution 4.0 International License.
Read Full License

Additional Declarations: No competing interests reported.

In Vitro and *In Silico* Evaluation of the Efficacy and Safety of a Ghanaian Herbal Medicine for the Treatment of Onchocerciasis and African Trypanosomiasis

Barbara Zenabu Anibea[#], Eric Coffie[#], Daniel Moscoh Ayine-Tora[#], Theresa Manful Gwira[$ɣ], Dorcas Osei-Safo[#‡]

[#]Department of Chemistry, University of Ghana
[$]West African Centre for Cell Biology of Infectious Pathogens, University of Ghana
[ɣ]Department of Biochemistry, Cell and Molecular Biology, University of Ghana

[‡]Corresponding author: dosei-safo@ug.edu.gh; +233208169376

Abstract

Background: This study investigated the anti-onchocercal and antitrypanosomal properties of a Ghanaian herbal medicine (NTD-O2) and its medicinal plant constituents, *Xylopia aethiopica* fruits and *Bambusa vulgaris* leaves, with the aim of addressing the therapeutic potential and safety of a herbal medicine against Onchocerciasis and Animal African Trypanosomiasis in Ghana.

Methods: Extracts from NTD-O2 and the medicinal plants were tested against *Onchocerca ochengi* and *Trypanosoma brucei brucei in vitro*. Bioassay-guided fractionation, spectroscopic and spectrometric techniques identified bioactive compounds, while *in silico* methods explored their possible mechanisms of action.

Results: NTD-O2 extracts achieved 100% inhibition of adult male *O. ochengi* worm motility, with moderate activity against adult female worms. Additionally, the extracts demonstrated promising antitrypanosomal activity (IC_{50} = 9.44 µg/mL and 10.68 µg/mL) against the positive control, diminazene aceturate (IC_{50} = 0.13 ± 0.02 µg/mL). The active compound found in the NTD-O2 extract was bis(4-methylheptyl) phthalate. On the contrary, the compounds isolated from *X. aethiopica* – ent-kaur-16-en-19-oic acid, xylopic acid, and ent-kaur-16-en-15-one-19-oic acid – and the long chain carbonyl compounds from *B. vulgaris* were inactive (IC_{50} = >100 ± 0.46 µg/mL). These results were corroborated by *in silico* analysis.

Conclusion: The findings highlight significant variability in the chemical composition and bioactivity of the herbal medicine NTD-O2 and its plant constituents. Given the health risks linked to the ingestion of phthalate derivatives, it is essential to conduct regular assessments of the quality and safety of herbal medicines to ensure consumer protection.

Keywords: Herbal medicine, safety, *Xylopia aethiopica*, *Bambusa vulgaris*, Onchocerciasis, Animal Trypanosomiasis, phthalate

Background

Rooted in indigenous knowledge and cultural beliefs, herbal medicine (HM) has been the cornerstone of human healthcare for centuries and continues to offer readily available and affordable healthcare to approximately 80% of the

population in developing countries. Practically, for most indigenous people living in remote rural areas with limited access to conventional medical services, HM is the only treatment option.[1] Besides, over the past three decades, many developed countries have widely embraced the use of HM to promote healthier living.[2-4] While HM is perceived to have less adverse effects, they are commonly used as self-care treatments and are unregulated, posing huge safety risks for consumers. In response to these challenges, coupled with the recognition of their enormous value for achieving universal healthcare, the World Health Organization (WHO) established technical guidelines and standards to ensure the safety, efficacy and quality control of HM.[5-8]

HM is a significant aspect of Ghana's cultural heritage and its development over the years is well documented.[9-13] Since 2012, the practice has been approved by the government for integration into the mainstream healthcare system,[14] resulting in a wide range of HM products on the Ghanaian market for treating a variety of disease conditions. The Ghana Food and Drugs Authority (FDA) is mandated to approve and register such products based on efficacy, safety and clinical data. The rational use of HMs has largely been supported by research output on the scientific validation of their efficacy claims. However, the challenge is that many of the FDA-approved products cover common ailments such as malaria, anaemia, cough, and asthma, unlike remedies for conditions like the neglected tropical diseases (NTDs) due to lack of access to efficacy testing platforms.[12] Hence, many people affected by

NTDs are exposed to unapproved HM, a situation with the potential for serious safety and efficacy implications and therefore requires urgent scientific validation for better healthcare outcomes.

Onchocerciasis, commonly known as river blindness, is a parasitic disease caused by the filarial nematode *Onchocerca volvulus* and transmitted through the bite of infected female blackflies (*Simulium spp.*).[15] The disease is responsible for a range of skin and eye-related morbidities including irreversible blindness.[16] Onchocerciasis is reported among the NTDs that remain endemic in several Ghanaian communities after more than 18 rounds of annual mass drug administration with ivermectin.[17] Our interaction with the Ghana Federation of Traditional Medicines Practitioners Association (GHAFTRAM) revealed the existence and high patronage of HM by affected people in NTD-endemic communities.[18] As part of efforts to contribute to the promotion and development of these remedies, we sought to conduct a comparative investigation of a HM used in treating onchocerciasis (NTD-O2) and its medicinal plant constituents. Thus, the constituents of NTD-O2 and its component medicinal plants (*Xylopia aethiopica* fruits and *Bambusa vulgaris* leaves) were extracted and separately screened for anti-onchocercal activity against *Onchocera ochengi*. Bioassay-guided fractionation was used to identify the bioactive constituents. Structural elucidation techniques involving spectroscopic and spectrometric methods were used to characterize the chemical constituents. The possible mechanisms of action of the compounds were further determined by *in silico* techniques.

Animal African trypanosomiasis (AAT), unlike human trypanosomiasis (sleeping sickness,) continues to be highly neglected primarily due to limited resources and global attention directed towards human disease control. While AAT causes huge economic loses in livestock production, coupled with the direct effects on human health, the financial incentives for developing veterinary drugs for livestock disease are often low, resulting in limited treatment options.[19] According to Tweneboah et al.[20], information on the current situation of AAT in Ghana is scanty due to neglect even at the national level. In our earlier work,[18] we demonstrated that a chemical constituent of NTD-B4, a herbal medicine used against schistosomiasis, was effective against *Trypanosoma brucei brucei* compared to the standard antitrypanosomal drug, diminazene aceturate. Hence, NTD-O2 extracts and compounds as well as those from the medicinal plants were subjected to antitrypanosomal activity screening against *Trypanosoma brucei brucei*.

To ensure herbal medicines can serve as viable alternatives to conventional treatments for parasitic infections, regular screening is essential. This process guarantees quality assurance, efficacy, and safety, thereby enhancing their credibility and protecting consumers.

Material and methods

Herbal Medicine and Plant Materials

NTD-O2 is a Ghanaian herbal medicine used in the treatment of onchocerciasis. It was prepared from two medicinal plants, the dry fruits of *Xylopia aethiopica* and the fresh leaves of *Bambusa vulgaris* and provided by

GHAFTRAM for the study. In addition to the herbal medicine (NTD-O2), the constituent plant materials were also collected and analyzed separately. Dry *X. aethiopica* fruits were sourced from Nima Market, Accra, and fresh *B. vulgaris* leaves from the University of Ghana campus. Both were identified by Mr. Patrick Ekpe and assigned voucher numbers BZA 001 and BZA 002 at the Ghana Herbarium, Department of Plant and Environmental Biology, University of Ghana.

Extraction and Isolation

NTD-O2 was subjected to the protocol described by Twumasi et al. (2020)[18] with slight modification. Briefly, a total of 3.8 litres of NTD-O2 was extracted in 500 mL aliquots with equal volumes of HPLC-grade dichloromethane (DCM) and n-butanol (n-BuOH) sequentially. For each aliquot, the procedure was repeated three times to yield the corresponding crude extracts NTD-O2-DCM (7 g) and NTD-O2-BuOH (25 g). The NTD-O2-BuOH extract was then sequentially fractionated with hexane, DCM, Ethylacetate (EtOAc) and Methanol (MeOH). Each fraction was concentrated under vacuum and refrigerated at 4 °C for about 72 h to facilitate precipitation of solids. The EtOAc fraction gave a yellow-brown solid (O2-F3-S, 5 g) and was purified over a column of 60 g of silica gel (130-270 Å mesh, SIGMA-ALDRICH) eluted with petroleum ether (PE) and EtOAc to yield compound **1** (O2-F3-S, 8 mg) and compound **2** (O2-F3-ML, 20 mg).

Dried powder (1 kg) of *X. aethiopica* fruits and fresh leaves of *B. vulgaris* (674.0 g) were separately extracted continuously via cold percolation with Petroleum Ether (PE) for 72 hours. The solvent was removed under reduced pressure to give an oily crude extract for *X. aethiopica* (XA/PE, 30.8 g) and greenish paste crude for *B. vulgaris* (BL/PE, 10 g). XA/PE (10 g) was chromatographed over a column of silica gel (120 g) and eluted with PE/EtOAc (v/v = 10:0, 9:1, 8:2, 6:4, 1:1, 0:10) and EtOAc/MeOH (9.5:0.5). A total of 315 eluates (v = 20 mL) were obtained and pooled together based on TLC profile into 13 fractions (1-13). Upon evaporation under vacuum, fractions 1-12 were oily while fraction 13 was a powdery solid. Following refrigeration at 4 °C for about 72 h, fractions 2-5 generously precipitated colourless crystals (BZA 01, 5 g), fractions 11-12 precipitated another set of colourless crystals (BZA 02, 4.7 g), while fraction 9 precipitated a greenish powder (BZA 05, 200 mg). *B. vulgaris* (BL/PE, 7 g) was also subjected to silica gel column chromatography using a similar protocol as described above to yield 2 compounds, a white powder (BL 2, 10 mg) and yellow gum (BL 4, 3 mg). Thin-layer chromatography (TLC) was conducted on silica gel 60 F_{254} (Merck) pre-coated aluminium foil slides, visualized with UV light (254 and 364 nm) and anisaldehyde spray reagent heated to 110 °C.

Structure elucidation techniques

^{1}H and ^{13}C NMR spectra were recorded on a Brüker, 500 MHz spectrometer in $CDCl_{3,}$ with chemical shifts referenced to tetramethyl silane. LC-MS analysis was performed using an Agilent HPLC system equipped with a

Kinetex Core C18 column (2.6 µM, 3 x 50 mm, 100 Å) at 40 °C. The mobile phase consisted of acetonitrile-ethyl acetate 9:1 eluted under gradient conditions at 0.7 mL/min. Injection volume was 2 µL, and the mass spectra were obtained using electrospray ionization (ESI) and atmospheric pressure chemical ionization. GC-MS analysis was conducted on a Perkin Elmer GC Clarus 580 with electron impact ionization at 70 eV and helium gas at 1 mL/min. National Institute Standard and Technology (NIST) library was employed in compound identification. Infra-red spectral data was acquired neat on a Perkin Elmer FTIR spectrometer using the attenuated total reflectance technique. MS analyses of samples were performed using an Agilent 1100 Autosampler instrument with ESI at 3.5 kV and a Thermo Q-Exactive orbitrap instrument. X-ray crystallography measurements were done on a Brüker ECO D8 diffractometer, with data collection at 296.15 K and the structure solved with the olex2.solve and refined with and refined with the ShelXL.

In vitro **anti-onchocercal assay**

Stock solution (20 mg/mL) of NTD-O2-DCM and NTD-O2-BuOH in DMSO were tested on the worms and larvae of *O. ochengi* as previously described.[18, 23] Auranofin (10 µM) was used as the positive control while 2% of DMSO served as the negative control. The viability of the adult female worms was evaluated biochemically by visually assessing the percentage inhibition of formazan production after incubating the nodules in 500 µL of 0.5 mg/mL

MMT.[24] A loss of the characteristic blue coloration in the worms indicated worm death. A test sample was classified as active if it inhibited more than 90% of female worm motility or formazan production, moderately active if it caused 50–89% inhibition, and inactive if inhibition was below 50%.

In vitro Anti-trypanosomal assay

Bloodstream forms of *T. brucei brucei* were used in this study due to their similarity to the human-infective forms, *T. b. rhodesiense* and *T. b. gambiense*.[25] The protocol employed is as previously described.[18] Briefly, crude extracts were dissolved in 100% DMSO to make a 20 mg/mL stock, then diluted to 2 mg/mL in sterile distilled water for testing. Isolated compounds (BZA 01, BZA 02, BZA 05 from *X. aethiopica*; BL 2 and BL 4 from *B. vulgaris*) were prepared similarly. Trypanosome cells in media without treatment served as the negative control, while diminazene aceturate (DA) was the positive control. Wild-type bloodstream forms of *T. b. brucei* (GuTat 3.1 strain) were cultured in Hirumi's Modified Iscove's Medium-9 (HMI-9),[26] supplemented with 1% penicillin-streptomycin and 10% heat-inactivated fetal bovine serum (Gibco). The cultures were maintained at 37 °C with 5% CO_2. An Alamar blue assay was used to test the crude extracts and compounds.[27] Serial dilutions (100 to 0.1953 µg/mL) were prepared in 96-well plates. Log-phase trypanosomes were added, and the plates were incubated for 72 hours at 37°C in 5% CO_2. A final concentration of 44 µM of resazurin sodium salt (Sigma-Aldrich) in phosphate buffered saline was then added to each well,

plates were incubated for additional 5 h and the absorbance measured at 570 nm using the Varioskan Lux Elisa plate reader (ThermoFisher Scientific, USA). Each test was done in triplicate, with three technical replicates.

Statistical analysis

Plate readouts from the Alamar blue assay were evaluated using non-linear regression analysis ($\log_{10}$ inhibitor versus response-variable slope) to assess growth inhibition. This analysis was performed using GraphPad Prism version 8.0.1. The IC_{50} values of the test samples were determined from three biological replicates, each conducted in triplicate.

***In silico* studies**

In silico studies were performed on compounds isolated from *X. aethiopica* and *B. vulgaris* in the current study and those reported in literature to validate the outcomes of the *in vitro* anti-onchocercal and antitrypanosomal assays. These studies included predictions of pharmacodynamics (PD) and pharmacokinetics (PK), as well as molecular modelling of compounds.

Selection of Protein Targets

For *O. ochengi,* the typical protein targets selected were glutathione S-transferase and glutamate-gated chloride ion channel. In the case of *T. brucei brucei,* ornithine decarboxylase was chosen as the protein target.[28-31] Ornithine Decarboxylase is a crucial enzyme-dependent growth factor, playing a vital role for the parasite through the formation of polyamine putrescine, a molecule important in the pathway for the production of trypanothione.[32]

Prediction of the PD and PK of the Compounds

The SwissADME server was used to predict PD and PK properties of the isolated compounds.[33]

Measurement of PK Properties and Drug-Likeness

The SwissADME server was further utilized to determine the physicochemical descriptors of the compounds, as well as to define their PK properties and drug-like nature. The Brain or Intestinal Estimated Permeation (BOILED-Egg) model was employed to intuitively evaluate passive human gastrointestinal absorption (HIA) and blood-brain barrier (BBB) penetration. This model was also used to compute the lipophilicity and polarity of the compounds.

Modelling of compounds

The compounds, both isolated in the current study and those reported in literature, were docked to the crystal structure of the Glutathione S-Transferase (Protein Data Bank (PDB) ID: 1TU8, resolution 1.80 Å)[32] and Glutamate-gated chloride channel (GluCl) (PDB: 3RHW, resolution 3.26 Å), which are protein targets for onchocerciasis. Additionally, these compounds were docked against ornithine decarboxylase (PDB ID: 1F3T, resolution 2.00 Å),[34] a protein target for trypanosomiasis. The crystal structures of co-crystallized ligands were obtained from PDB.[35, 36] These structures were prepared by removing the co-crystallized ligands and adding the hydrogen atoms using the Scigress version FJ 2.6 program. The binding pocket center of the Glutathione S-Transferase was identified by fitting the atoms of the co-crystallised ligand 5-hexyl Glutathione (x = 2.570, y = 0.814, z = 49.968) with a radius of 10 Å. Similarly, the binding pocket centre of glutamate-gated chloride channel was defined by the position of the atoms of co-crystallized ligand ivermectin (x = 12.675, y = 95.052, z = 24.998) with a radius of 10 Å. The binding pocket centre of ornithine decarboxylase was identified by the position of the phosphorus atom of the co-crystallised ligand pyridoxal-5'-phosphate (coordinates: x = 26.206, y = 15.614, z = 3.800) and a radius of 10 Å. To validate the predicted binding modes and relative energies of the ligands, the GoldScore (GS)[37], ChemScore (CS)[38,39], ChemPLP[40] and Astex statistical potential (ASP)[41] scoring functions were implemented using the GOLD v5.4 software suite.

Results and discussion

In vitro anti-onchocercal and antitrypanosomal activity of NTD-O2

The results of the *in vitro* anti-onchocercal and antitrypanosomal assays are summarized in **Table 1**. In primary screens against *O. ochengi*, both the dichloromethane extract of NTD-O2 (NTD-O2-DCM) and the butanol extract (NTD-O2-BuOH) at 200 µg/mL, as well as the positive control, auranofin at 10 µM showed 100 ± 0% inhibition of the adult male worm. This indicates that the crude extracts of the herbal medicine at the specified concentration were as effective as the control against the adult male worm. However, while auranofin maintained the same level of activity against the adult female worm, the extracts demonstrated moderate activity, with 61.0 ± 1.8% and 56.6 ± 4.4% inhibition, respectively. Due to the moderate activity against the female worm, which is a critical criterion for advancing to secondary screens, the extracts were not selected for further testing against the parasites.

In contrast, the antitrypanosomal assay results were promising for both extracts, with IC_{50} values of 10.68 ± 2.54 µg/mL for NTD-O2-DCM and 9.44 ± 1.88 µg/mL for NTD-O2-BuOH against *T. b. brucei*. The positive control, diminazene aceturate, recorded an IC_{50} value of 0.13 ± 0.02 µg/mL (**Table 1**). While the extracts were less potent than diminazene aceturate, their IC_{50} values are still within a range that suggests possible optimization or application in combination therapies to enhance efficacy.

Table 1: Anti-onchocercal and antitrypanosomal screening of NTD-O2 and its medicinal plant isolates

No.	Test sample	Cytotoxic	Anti-onchocercal activity against adult worms of *O. ochengi*		Antitrypanosomal activity against bloodstream forms *T. b. brucei*
			%Inhibition of males (5 days)	%Killing of females (7 days)	IC_{50} (µg/mL) Mean ± SD
			NTD-O2		
1	NTD-O2-DCM	No	100±0	61.0±1.8	10.68 ± 2.54
2	NTD-O2-BuOH	No	100±0	56.6±4.4	9.44 ±1.88
3	Auranofin (10 µM)	N/A	100±0	100±0	N/A
4	iminazene acetura	N/A	N/A	N/A	0.13 ± 0.02
			Isolates from NTD-O2-BuOH		
1	O2-F3-S		N/A		100 ± 0.46
2	O2-F3-ML		N/A		1.1 ± 0.3
3	iminazene acetura		N/A		0.18 ± 0.01
			Isolates from medicinal plants		
1	BZA 01		N/A		>100 ± 0.46
2	BZA 02		N/A		ND
3	BZA 05		N/A		>100 ± 0.46
4	BL2		N/A		>100 ± 0.46
5	BL4		N/A		>100 ± 0.46

6	iminazene acetura	N/A	0.18 ± 0.01

N/A = Not applicable; N/D = Not determined; Calculated adult worm activity responses were done in quadruplicates, IC_{50} values represent mean averages of 3 biological replicates.

The higher activity results of the antitrypanosomal assay informed a bioassay-guided fractionation and isolation of compounds from NTD-O2 and its medicinal plants, *X. aethiopica* and *B. vulgaris*. NTD-O2-BuOH was prioritized over NTD-O2-DCM due to its higher IC_{50} value.

Antitrypanosomal activity of isolates from NTD-O2-BuOH

NTD-O2-BuOH was sequentially fractionated with hexane, dichloromethane (DCM), ethyl acetate (EtOAc) and methanol (MeOH) to obtain the corresponding fractions. Isolates from the hexane and DCM fractions encountered solubility issues in dimethyl sulfoxide (DMSO), precluding their assay results. Additionally, attempts to purify the MeOH fraction were unsuccessful. Hence, only isolates O2-F3-S and O2-F3-ML from the EtOAc fraction were evaluated for their antitrypanosomal activity.

O2-F3-S exhibited limited bioactivity, with an IC_{50} value of 100 ± 0.46 µg/mL. In contrast, O2-F3-ML demonstrated significant antitrypanosomal activity, with an IC_{50} value of 1.1 ± 0.3 µg/mL. When compared to the standard antitrypanosomal agent, diminazene aceturate, which had an IC_{50} of 0.18 ± 0.01 µg/mL, O2-F3-ML shows a comparable efficacy.

The cytotoxicity (CC_{50}) of O2-F3-ML was determined to be 100 µg/mL, whereas diminazene aceturate exhibited a CC_{50} of 36 ± 2 µg/mL against the standard phenylarsine oxide, which has a CC_{50} value of 1.0 ± 0.1 µg/mL. This indicates that the cytotoxicity of O2-F3-ML is moderate. Consequently, the selective index (SI) was calculated to be 89 ± 25 for O2-F3-ML and 203 ± 22 for diminazene aceturate. These findings suggest that O2-F3-ML possesses notable antitrypanosomal activity and hence was subjected to structure elucidation.

Structure Elucidation of O2-F3-ML

Sample O2-F3-ML was obtained as a yellowish oil with a retention factor (Rf) of 0.75 on TLC developed in hexane and acetone (7:3). The IR data gave absorptions at 2958 $cm^{-1,}$ 2927 cm^{-1} and 2858 cm^{-1} (C-H), 1726 cm^{-1} (C=O) and 1610 cm^{-1} (aromatic C=C). The ^{1}H-NMR spectrum (**Supplementary information Figure S1**) exhibited a typical AA'BB' system at H-4/H-4' (δ_H 7.53, dd, J = 3.3 and 5.7 Hz, 2H) and H-3/H-3' (δ_H 7.70, d, J = 3.3 Hz, 2H) supporting an ortho-disubstituted benzene ring with identical substituents in both positions. Signals were seen at δ_H 0.90 (d, J = 5.5 Hz, 3H) for the secondary methyl protons H-12/H-12' and δ_H 0.91 (t, J = 13.8 Hz, 3H) for the terminal methyl protons H-11/H-11'. A string of multiplets at δ_H 1.31, δ_H 1.35, δ_H 1.42, δ_H 1.68 and δ_H 4.22, was suggestive of methylene groups, with the latter linked to the ester. The ^{13}C NMR and DEPT 135 spectra (**Supplementary information Figures S1, S2**) revealed resonances for

methyl signals δ_C 11.1 (C-12/C-12') and δ_C 14.2 (C-11/C-11'), methylene carbon signals at δ_C 23.1 (C-10/C-10'), δ_C 23.9 (C-9/C-9'), δ_C 29.0 (C-8/C-8'), δ_C 30.5 (C-7/C-7'), and an sp^3 methine carbon signal at δ_C 38.9 (C-6/C-6'). The sp^3 oxygenated carbon (C-5/C-5') appeared at δ_C 68.4. Further, there were aromatic methine carbon peaks at δ_C 128.9 (C-4/C-4'), δ_C 131.0 (C-3/C-3') along with a quaternary aromatic carbon peak at δ_C 132.6 (C-2/C-2') and a carbonyl carbon at δ_C 167.9 (C-1/C-1') due to an ester moiety.

HMBC spectral data provided correlations between the methyl protons at δ_H 0.90 (H-12) and δ_C 23.1 (C-10), 23.9 (C-9) and 29.0 (C-8). Correlations H-5/C-8, C-1 established the ester linkage and H-12/C-6, C-7, C-9; H-5/C-6 confirmed the branched position of the side chain. The mass spectrum from the GC-MS analysis displayed fragment peaks at m/z 29, 43, 57, 71, 83, 149, 167, and 279, characteristic of alkyl phthalates (**Supplementary information Figure S4**). The molecular ion peak occurred at m/z 390 and the base peak at m/z 149, representing a protonated phthalate anhydride. Based on these assignments, the structure of O2-F3-ML was deduced as bis(4-methylheptyl) phthalate (**Fig. 1**).

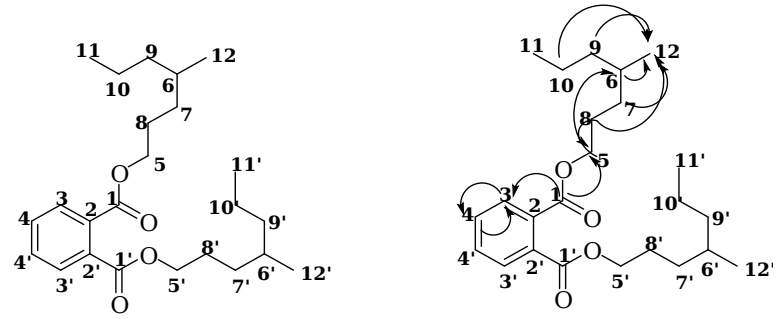


Figure 1 : Chemical structure and HMBC representation of Bis(4-methylhepthyl)phthalate

Phthalates and their derivatives are widely recognized as environmental contaminants due to their extensive industrial use. Prolonged or excessive exposure to these compounds has been associated with significant health risks in humans, including endocrine disruption, metabolic disorders, cancer, reproductive health issues and developmental challenges in children.[42, 43] In contrast, phthalates have also been reported in natural sources such as plants, bacteria, and fungi, demonstrating diverse biological potential such as antitumor, cytotoxic, allopathic, larvicidal, antiviral and anti-inflammatory properties.[42]

In vitro antitrypanosomal activity of the medicinal plant isolates

Compounds BZA 01, BZA 05, BL 2 and BL 4 recorded an IC_{50} value of >100 ± 0.46 µg/mL and hence, did not demonstrate any antitrypanosomal activity.

BZA 02, on the other hand, could not be assayed due to challenges with solubility in DMSO.

Structure elucidation of the medicinal plant isolates

BZ 01

BZA 01 was obtained as colourless crystals that appeared as an orange spot when visualized in anisaldehyde with Rf of 0.65 on TLC developed in PE: EtOAc (10:1). The IR spectrum showed characteristic peaks at 1726.56 cm^{-1} for carbonyl and 1687.91 cm^{-1} for unsaturation (C=C).

The ^{13}C NMR and DEPT 135 spectra (**Supplementary information Figures S5, S6**) exhibited 20 carbon signals sorted by the DEPT experiment into 5 quaternary carbons (including a carboxylic carbon at δ_C 185.1 (C-3) and an alkene carbon (C-16) at δ_C 155.8), 3 methine carbons, 2 tertiary methyl carbons and 10 methylene carbons, which were consistent with a kaurenoic acid skeleton. In the ^{1}H NMR spectrum (**Supplementary information Figure S7**), signals for the olefinic protons H20a (d, δ_H 4.80, 1H) and H-20b (d, δ_H 4.74, 1H) and tertiary methyls H-4 (s, δ_H 1.24, 3H) and H-7 (s, δ_H 0.95, 3-H) supported the presence of kaurenoic acid. HMBC correlations between C-3/H-4, H-5 established the position of the carboxylic acid while the exocyclic alkene was fixed by correlations from C-15, C-16, C-17/H-20a, H-20b.

In addition, the crystal structure revealed an empirical formula of $C_{20}H_{30}O_2$ and M =302.43 g/mol: $C_{20}H_{30}O_2$ had an orthorhombic, space group $P2_12_12_1$ (no. 19), a = 12.3081(7) Å, b = 23.8205(14) Å, c = 24.0947(14) Å, V = 7064.2(7) Å^3, Z = 4, T = 296.15 K, μ(MoKα) = 0.071 mm^{-1}, *Dcalc* = 1.134 g/cm^3, 323447 reflections measured (4.09° ≤ 2Θ ≤ 57.286°), 18029 unique (R_{int} = 0.1149, R_{sigma} = 0.0468). The final R_1 was 0.0728 (I > 2σ(I)) and wR_2 was 0.1523 (**Fig. 3**). Consequently, the structure of BZA 01 was determined as ent-kaur-16-en-19-oic acid, previously isolated from *X. aethiopica*.[21]

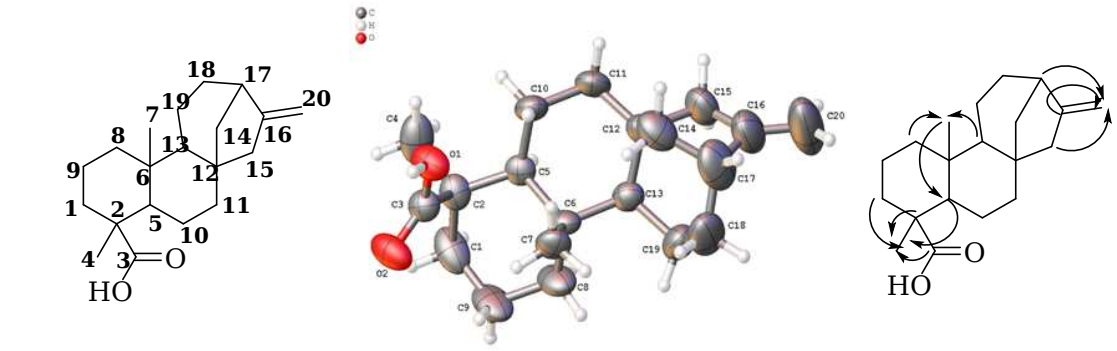


Figure 2: Chemical and Crystal structure, and HMBC representation of ent-kaur-16-en-19-oic acid

BZ 02

BZA 02 was also obtained as colourless crystals. On TLC developed in PE: EtOAc (10:2), the Rf was 0.40 and appeared purple in anisaldehyde spray reagent. The IR spectrum revealed absorption bands of hydroxyl (3280.90 cm-

^{1}), carbonyl (1724.65 cm^{-1}) and olefinic C=C stretch (1687.91 cm^{-1}). ^{1}H and ^{13}C NMR (**Supplementary information Figures S8, S9**) data were similar with those of BZA 01, indicating structural similarities. The significant difference was an additional quaternary carbon peak, δ_C 171.8 (C-21) in BZA O2 due to an ester carbonyl peak at δ_C 171.8 (C21) and the acetyl carbon at δ_C 21.7 (C-22). The position of the ester group at C-19 was supported by the HMBC correlations of H-20a and H-20b to C-16, C-18 and C-19, suggesting that BZA 02 is xylopic acid, also previously isolated from *X. aethiopica*. [22]

X-ray crystallography data gave an empirical formula of $C_{22}H_{32}O_4$ and M = 360.47 g/mol. BZA 02 came out as an orthorhombic shaped crystal with space group $P2_12_12_1$, a = 11.0960(5) Å, b = 11.8948(7) Å, c = 14.9745(8) Å, V = 1976.40(18) Å3, Z = 4, T = 296.15 K, μ(MoKα) = 0.082 mm-1, Dcalc = 1.211 g/cm3, 20732 reflections measured (5.02° ≤ 2Θ ≤ 53.028°), 4083 unique (Rint = 0.0979, Rsigma = 0.0772) as well as a final R1 was 0.0460 (I > 2σ(I)) and wR2 was 0.0980 which were used to calculate and confirm the structure of BZA 02 as xylopic acid (**Fig. 3**).

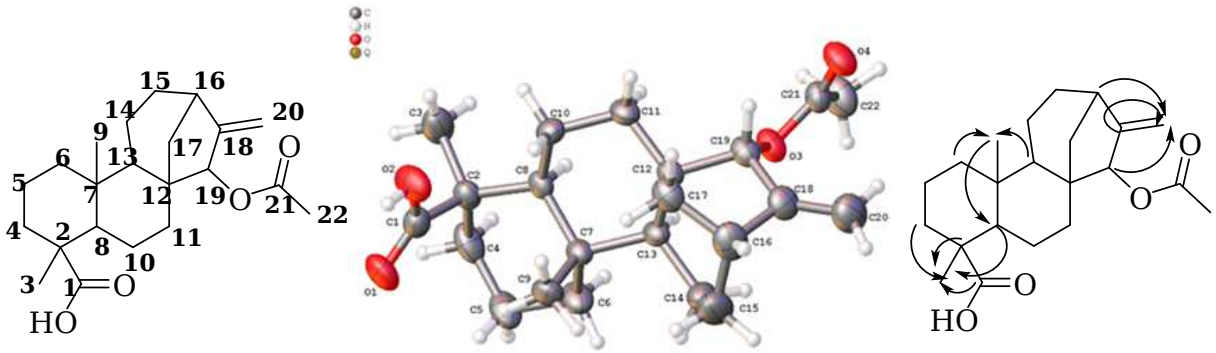
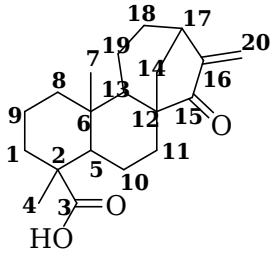


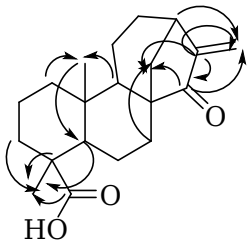
Figure 3: Chemical and Crystal structure, and HMBC representation of Xylopic acid

BZ 05

BZA 05 was isolated as a fine green powder and exhibited IR and NMR spectra closely resembling those of BZA 01. However, notable differences included a characteristic IR absorption band at 1724.36 cm^{-1}, indicative of a ketone, and a significant downfield shift in the ^{13}C NMR spectrum for carbon C-15 — from δ_C 49.1 in BZA 01 to δ_C 210.5 in BZA 05 — consistent with ketone functionality (**Supplementary Information Figure S10**). HMBC correlations between C-15 and H-20a, H-20b and H-14 were supportive of the assignment. The proposed structure was corroborated with the MS data analysis which exhibited an M+1 peak at m/z 317.21 accompanied with fragments at m/z 299.20 and 271.2 (**Supplementary Information Figure**

S11). Hence, the structure BZA 05 was deduced as ent-kaur-16-en-15-one-19-oic acid, with a molar mass of 316 g/mol (**Fig. 5**).





$C_{20}H_{28}O_3$
BZA05
(ent-kaur-16-en-15-one-19-oic acid)
Mw=316.44 g/mol

HMBC of BZA05

Figure 4: Chemical structure of ent-kaur-16-en-15-one-19-oic acid and HMBC representation of ent-kaur-16-en-15-one-19-oic acid

BL 2 and BL 4a

Compound BL 2 was isolated as white powder. Its IR spectrum exhibited characteristic absorption bands for C–H stretching at 2914.8 cm^{-1} and 2848.4 cm^{-1}, a carbonyl group at 1733.8 cm^{-1}, and an olefinic C=C stretch at 1683.9 cm^{-1}. In the ^{13}C NMR spectrum (**Supplementary Information Figure S12)**, signals corresponding to carbonyl carbons were observed at δ_C 195.0 (aldehyde) and δ_C 173.7 (ester). Olefinic carbons resonated at δ_C 155.2, 143.6, 134.9, and 124.1. An oxygenated carbon appeared at δ_C 64.1, while the remaining signals, ranging from δ_C 39.3 to δ_C 14.0, indicated the presence of a long alkyl chain. This was further supported by a series of multiplets in the upfield region of the ^1H NMR spectrum (δ_H 2.34–0.88). An aldehydic

proton was observed at δ_H 9.36, and signals at δ_H 6.44 and 5.12 were attributed to olefinic protons (**Supplementary Information Figure S13)**.

Compound BL 4, a yellow gum, showed IR absorption bands at 2916.4 cm^{-1} and 2849 cm^{-1} (C–H stretching) and a carbonyl absorption at 1702.4 cm^{-1}. The ^{13}C NMR spectrum (**Supplementary Information Figure S14)** displayed a carbonyl resonance at δ_C 180.5, with additional signals between δ_C 34.5 and 14.5, while the ^{1}H NMR spectrum (**Supplementary Information Figure S15)** showed multiplets in the δ_H 2.34–0.88 range. These spectral features are consistent with the structure of a fatty acid.

Molecular Modelling

To validate the results of the *in vitro* antitrypanosomal screening, *in silico* analysis was conducted to provide further understanding of the biological mechanisms involved. Physicochemical descriptors such as MW (g/mol), log *P*, HD, HA. RB, Lipinski, Ghose and Veber of the isolated compounds - bis(4-methylheptyl) phthalate, ent-kaur-16-en-19-oic acid, xylopic acid and ent-kaur-16-en-15-one-19-oic acid were determined as shown in (**Supplementary information Table S1**) to predict their individual ADME parameters. HA, HD, RB, log *P* and Lipinski values were within the drug-like chemical space. Likewise, MW was within the Known Drug Space (**Supplementary information Table S2**).

Co-crystallized ligands, including ivermectin (targeting glutathione S-transferase) and 5-hexyl glutathione (targeting the glutamate-gated chloride channel) for onchocerciasis, as well as pyridoxal-5-phosphate and doxycycline (targeting ornithine decarboxylase) for trypanosomiasis, were used as references to predict their functional scores against the respective target sites. Subsequently, the compounds were docked, together with and a wide range of compounds reported in the literature to have been isolated from *X. aethiopica* (**Supplementary information Table S4**).

Modelling against glutathione S-transferase (Onchocerciasis)

The co-crystallized ligand of glutathione S-transferase (**Supplementary Information Figure S16**) was first docked to generate root mean square deviation (RMSD) values for the heavy atoms. ASP obtained an average RMSD of 2.1366, PLP = 5.1415, CS = 1.6224, and GS = 1.9383. CS and GS showed stronger prediction power of scoring functions against the target (**Supplementary information Table S3**). The modeling showed that the compounds occupy the hydrophobic binding pockets with a plausible binding mode. In comparison to the standard drug ivermectin, the binding affinity score for bis(4-methylheptyl) phthalate was remarkably high. Its carbonyl group formed a hydrogen bond with the side chain lysine 35 amino acid, and it also exhibited a π-π interaction with phenylalanine 8 (**Figure 5)**. Ivermectin exhibited a similar binding mode. In contrast, the kaurene diterpenoids ent-

kaur-16-en-19-oic acid, xylopic acid and ent-kaur-16-en-15-one-19-oic acid were inactive.

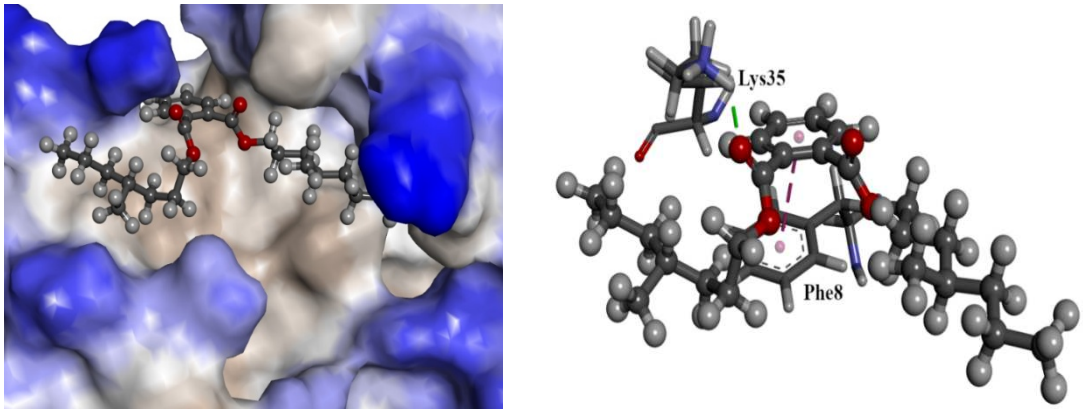


Figure 5: The docked configuration of bis(4-methylheptyl) phthalate in the binding site of glutathione S-transferase as predicted by ChemPLP (**A**) The ligand occupies the binding pocket. The protein surface is rendered. Blue depicts a hydrophilic region on the surface; brown depicts hydrophobic region and white shows neutral areas. (**B**) Hydrogen bonds are shown as green lines between bis(4-methylheptyl) phthalate and the amino acid Lysine 35 whiles π-π interaction between the molecule and phenylalanine 8.

Modelling against glutamate-gated chloride channel (Onchocerciasis)

Firstly, the co-crystallized ligand of the glutamate-gated chloride channel (**Supplementary information Figure S17)** was docked to generate average RMSD values for the heavy atoms as follows: ASP = 3.4741, PLP = 1.4928, CS = 1.4232, and GS = 1.7654, demonstrating stronger predictive power of the PLP and CS scoring functions against the target site (**Supplementary information Table S5**). The compounds occupied the hydrophilic binding pockets as a plausible binding mode, with 5-hexyl glutathione, the co-crystallized ligand, exhibiting the highest score, closely

followed by bis(4-methylheptyl) phthalate (**Supplementary information Table S6)**. Binding revealed hydrogen bond interactions between their respective carbonyl groups and the side chain hydroxyl groups of threonine, glutamine, and serine amino acids, with a typical illustration with asparagine amino acid (**Figure 6)**.

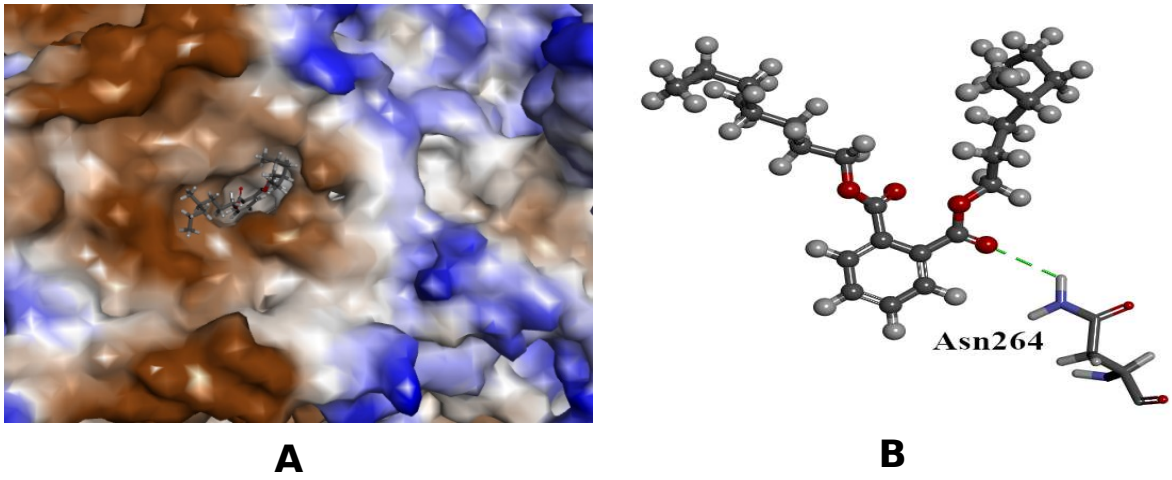
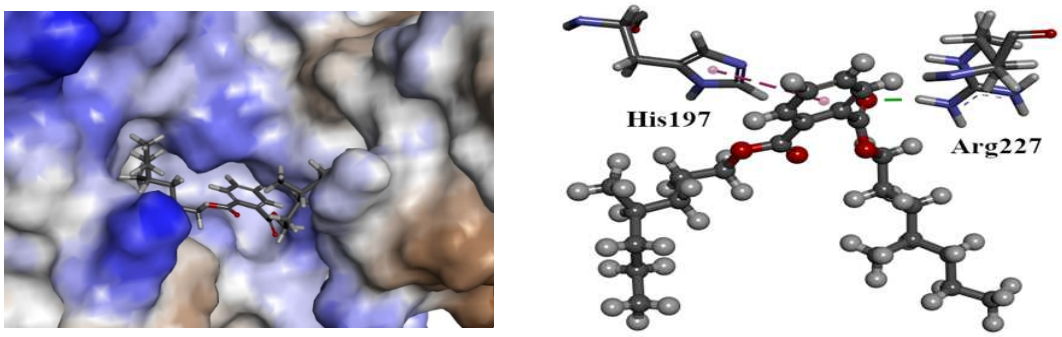


Figure 6: The docked configuration of bis(4-methylheptyl) phthalate in the binding site of glutamate-gated Cl ion channel as predicted by ChemPLP (**A**). The ligand occupies the binding pocket. The protein surface is rendered. Blue depicts a hydrophilic region on the surface; brown depicts hydrophobic region and white shows neutral areas. (**B**) Hydrogen bonds are shown as green lines between bis(4-methylheptyl) phthalate and the amino acid Asparagine 264.

Modelling against Ornithine Decarboxylase (Trypanosomiasis)

The co-crystallized ligands, pyridoxal-5-phosphate and doxycycline were initially docked with Ornithine Decarboxylase (**Supplementary information Figure S18**) to generate the RMSD values for the heavy atoms. ASP obtained an average RMSD of 0.4776, PLP = 1.5958, CS = 6.2696 and GS = 0.6362.

In this case, GS and ASP exhibited a very strong prediction power of scoring functions as compared to PLP and CS against the target (**Supplementary information Table S7)**. The modeled compounds again occupied the hydrophilic binding pockets with a plausible binding mode. As observed previously, bis(4-methylheptyl) phthalate demonstrated exceptionally high binding affinity with respect to the reference compounds, pyridoxal-5-phosphate and doxycycline **(Supplementary information Table S8**). It showed hydrogen bonding with the amine side chain of arginine while the phenyl moiety formed a π-π stack interaction with the imidazole side chain histidine (**Figure 7)**.



A **B**

Figure 7: The docked configuration of bis(4-methylheptyl) phthalate in the binding site of Ornithine decarboxylase as predicted by Goldscore (**A**). The ligand occupies the binding pocket. The protein surface is rendered. Blue depicts a hydrophilic region on the surface; brown depicts hydrophobic region and whites shows neutral areas. (**B**) Hydrogen bonds are shown as green lines between bis(4-methylheptyl) phthalate and the amino acids Arginine 227 whiles π-π interaction is shown with histidine.

Conclusion

The present study provides valuable insights into the pharmacological potential and safety considerations of the Ghanaian herbal formulation NTD-O2, traditionally used for the treatment of neglected tropical diseases. *In vitro* assays revealed that NTD-O2 possesses significant antitrypanosomal activity, with the isolated compound bis(4-methylheptyl) phthalate demonstrating potent efficacy against *T. brucei*. This activity was further supported by *in silico* molecular docking studies, which suggested favourable interactions with key parasitic targets, indicating a plausible mechanism of action.

However, the identification of bis(4-methylheptyl) phthalate—a compound widely recognized as a synthetic plasticizer and environmental contaminant—raises important concerns regarding the authenticity and safety of the observed bioactivity. The absence of comparable activity in the individual plant constituents, *Xylopia aethiopica* and *Bambusa vulgaris*, suggests that the therapeutic effects may not be attributable to the herbal components themselves but rather to external contamination introduced during processing or packaging. This finding underscores the critical need for stringent quality control measures in the preparation and evaluation of herbal medicines.

While the observed antitrypanosomal activity is promising, the potential toxicological implications of phthalate exposure cannot be overlooked. These

results highlight the dual necessity of validating the efficacy of traditional remedies while ensuring their safety through comprehensive chemical profiling and contamination screening. Future research should focus on optimizing the efficacy and safety profiles of promising compounds and exploring their potential in combination therapies.

List of abbreviations

Animal African trypanosomiasis	AAT
Astex statistical potential	ASP
ChemScore	CS
Diminazene aceturate	DA
Ghana Federation of Traditional Medicines Practitioners Association	GHAFTRAM
Ghana Food and Drugs Authority	FDA
Glutamate-gated chloride channel	GluCl
GoldScore	GS
Herbal medicine	HM
Human gastrointestinal absorption	HIA
Neglected tropical diseases	NTDs
Pharmacodynamics	PD
Pharmacokinetics	PK
Protein Data Bank	PDB
Root mean square deviation	RMSD
Selective index	SI
World Health Organization	WHO

Supplementary Information

The online version contains supplementary material available at...

Acknowledgements

The authors express their gratitude to the Department of Chemistry for NMR and X-ray data acquisition and New Zealand eScience Infrastructure (NeSI) high-performance computing facilities as part of this research funded jointly by the collaborating institutions and through the Ministry of Business, Innovation and Employment Research Infrastructure program. URL: https://www.nesi.org.nz. The *Trypanosoma brucei brucei* cell line (GUTat 3.1 strain) was originally obtained from the Department of Parasitology, Noguchi Memorial Institute for Medical Research, University of Ghana.

Ethics approval and consent to participate

Not applicable

Consent for publication

Not applicable

Availability of data and materials

The dataset supporting the conclusions of this article is included within the article and its additional file.

Competing interests

The authors have no competing interests.

Funding

This research was supported by Worldwide Universities Network Research Development Fund 2017 from the Worldwide Universities Network (UK) and

grant number 18-191 RG/CHE/AF/AC_G - FR3240303659 from The World Academy of Sciences.

Authors' contributions

BZA: Data acquisition and analysis; Writing – original draft, revision and final approval.

EC: Data acquisition and analysis; Writing – revision and final approval

DM: Supervision, Data acquisition and analysis; Writing –revision and final approval

TMG: Supervision, Data acquisition and analysis; Writing –revision and final approval

DOS: Funding acquisition, Conceptualization, Supervision, Data analysis. Writing – original draft, revision and final approval

References

1. World Health Organization (WHO), Traditional Medicine *EB124.R9* 2009.
2. Bodeker G, Kronenberg F. A public health agenda for traditional, complementary, and alternative medicine. Am J Public Health. 2002;92(10):1582–91
3. Ernst E. Prevalence of use of complementary/alternative medicine: a systematic review. *Bull World Health Organ*. 2000;78(2):252–7
4. Nissen N. Practitioners of Western herbal medicine and their practice in the UK: beginning to sketch the profession. *Complement Ther Clin Pract*. 2010;16(4):181–6
5. Flynn MAT, Maloff DA, Maloff B, Mutasingwa D, Wu M, Ford C, et al. Reducing obesity and related chronic disease risk in children and youth: a synthesis of evidence with ‘best practice’ recommendations. *Obes Rev.* 2006;6(1):7–16

6. Akerele O. WHO's traditional medicine programme: progress and perspectives. *WHO Chron*. 1984;38(2):76–81
7. World Health Organization (WHO). WHO traditional medicine strategy: 2014–2023. Geneva: WHO; 2013. Report No.: EB134/24.
8. World Health Organization. WHO traditional medicine strategy 2002–2005. Geneva, Switzerland: World Health Organization; 2002. Global review.
9. Twumasi PA. History of pluralistic medical systems: A sociological analysis of the Ghanaian case. *Issue*. 1979;9(3):29–34.
10. Essegbey GO, Awuni S. Herbal medicine in the informal sector of Ghana. In: Kraemer-Mbula E, Wunsch-Vincent S, editors. *The informal economy in developing nations: Hidden engine of innovation?* Cambridge: Cambridge University Press; 2016. p. 194–231.
11. Addae-Mensah I. Herbal medicine: does it have a future in Ghana? 1975.
12. Mintah SO, Archer M-A, Asafo-Agyei T, Ayertey F, Aboagye-Antwi P, Boamah D, et al. Medicinal plant use in Ghana: advancement and challenges. *Am J Plant Sci*. 2022;13(3):316–58.
13. Ministry of Health (MOH). Policy guidelines on traditional medicine development: Traditional medicine policy. Accra: Ministry of Health; 2005. p. 1–15.
14. Owoahene-Acheampong EVAS. Recognition and integration of traditional medicine in Ghana: A perspective. *Res Rev*. 2010;26(2):1–17.
15. Crawford KE, Hedtke SM, Doyle SR, Kuesel AC, Armoo S, Osei-Atweneboana M, Grant WN. Utility of the *Onchocerca volvulus* mitochondrial genome for delineation of parasite transmission zones. *bioRxiv*. 2019. doi:10.1101/2019.12.12.873612.

16. Brattig NW, Cheke RA, Garms R. Onchocerciasis (river blindness) – more than a century of research and control. *Acta Trop*. 2021;218:105677.
17. Chikezie FM, Veriegh FBD, Armoo S, Boakye DA, Taylor M, Osei-Atweneboana MY. Ongoing transmission of onchocerciasis in the Pru District of Ghana after two decades of mass drug administration with ivermectin and comparative identification of members of the *Simulium damnosum* complex using cytological and morphological techniques. *Parasit Vectors*. 2024;17(1):394.
18. Twumasi EB, Akazue PI, Kyeremeh K, Gwira TM, Keiser J, Cho-Ngwa F, et al. Antischistosomal, antionchocercal and antitrypanosomal potentials of some Ghanaian traditional medicines and their constituents. *PLoS Negl Trop Dis*. 2020;14(12):e0008919.
19. Pereira SH, Alves FP, Teixeira SMR. Animal trypanosomiasis: Challenges and prospects for new vaccination strategies. *Microorganisms*. 2024;12(12).
20. Tweneboah A, Rosenau J, Addo KA, Addison TK, Ibrahim MAM, Weber JS, et al. The transmission of animal African trypanosomiasis in two districts in the forest zone of Ghana. *Am J Trop Med Hyg*. 2024;110(6):1127–36.
21. Somova LI, Sinyangwe FO, Moodley K, Govender Y. Cardiovascular and diuretic activity of kaurene derivatives of *Xylopia aethiopica* and *Alepidea amatymbica*. *J Ethnopharmacol*. 2021;77:10.
22. Soh D, Ernestine N, Tchana Satchet EM, Defokou UD, Schneider B, Giovanni V, et al. Antiproliferative activity of semisynthetic xylopic acid derivatives. *Nat Prod Res*. 2022;36(5):1288–95.
23. Gyapong JO, Kumaraswami V, Biswas G, Ottesen EA. Treatment strategies underpinning the global programme to eliminate lymphatic filariasis. *Expert Opin Pharmacother*. 2005;6(2):179–200.
24. Nyongbela KD, Samje M, Awantu AF, Tiku TE, Cho-Ngwa F. Evaluation of anti-onchocercal activity of pseudopalmatine, a quaternary protoberberine alkaloid of *Enantia chlorantha* (Syn. *Annickia chlorantha*). *J Cameroon Acad Sci*. 2019;14(3).

25. Neuberger A, Meltzer E, Leshem E, Dickstein Y, Stienlauf S, Schwartz E. The changing epidemiology of human African trypanosomiasis among patients from nonendemic countries – 1902–2012. *PLoS One*. 2014;9(2):e88647.

26. Hirumi H, Hirumi K. Axenic culture of African trypanosome bloodstream forms. *Parasitol Today*. 1994;10(2):80–4.

27. Raz B, Iten M, Grether-Bühler Y, Kaminsky R, Brun R. Alamar blue assay to determine drug sensitivity of African trypanosomes (*T.b. rhodesiense* and *T.b. gambiense*) in vitro. *Acta Trop*. 1997;68:139–47.

28. Glendinning SK, Buckingham SD, Sattelle DB, Wonnacott S, Wolstenholme AJ. Glutamate-gated chloride channels of *Haemonchus contortus* restore drug sensitivity to ivermectin-resistant *Caenorhabditis elegans*. *PLoS One*. 2011;6(7):e22390.

29. Atif M, Estrada-Mondragon A, Nguyen B, Lynch JW, Keramidas A. Effects of glutamate and ivermectin on single glutamate-gated chloride channels of the parasitic nematode *H. contortus*. *PLoS Pathog*. 2017;13(10):e1006663.

30. Salinas G, Taylor DW. Molecular characterisation and localisation of an *Onchocerca volvulus* p-class glutathione-S-transferase. *Mol Biochem Parasitol*. 1994;66:10.

31. Perbandt M, Hoppner J, Betzel C, Walter RD, Liebau E. Structure of the major cytosolic glutathione S-transferase from the parasitic nematode *Onchocerca volvulus*. *J Biol Chem*. 2005;280(13):12630–6.

32. Jackson LK, Babbitt HB, Osterman AL, Goldsmith EJ, Phillips MA. Altering the reaction specificity of eukaryotic ornithine decarboxylase. *Biochemistry*. 2000;39(37):11.

33. Daina A, Michielin O, Zoete V. SwissADME: a free web tool to evaluate pharmacokinetics, drug-likeness and medicinal chemistry friendliness of small molecules. *Sci Rep*. 2017;7:42717.

34. Gladkova ED, Nechepurenko IV, Bredikhin RA, Chepanova AA, Zakharenko AL, Luzina OA, et al. The first berberine-based inhibitors of tyrosyl-DNA phosphodiesterase 1 (Tdp1), an important DNA repair enzyme. *Int J Mol Sci*. 2020;21(19).

35. Berman H, Henrick K, Nakamura H. Announcing the worldwide protein data bank. *Nat Struct Biol*. 2003;10(12):1.

36. Kitchen DB, Decornez H, Furr JR, Bajorath J. Docking and scoring in virtual screening for drug discovery: methods and applications. *Nat Rev Drug Discov*. 2004;3(11):935–49.

37. Jones G, Willett P, Glen RC, Leach AR, Taylor R. Development and validation of a genetic algorithm for flexible docking. *Mol Biol*. 1997;267:22.

38. Eldridge MD, Murray CW, Auton TR, Paolini GV, Mee RP. Empirical scoring functions: The development of a scoring function to estimate the binding affinity of ligands in receptor complexes. *J Comput Aided Mol Des*. 1997;11:21.

39. Miller PS, Smart TG. Binding, activation and modulation of Cys-loop receptors. *Trends Pharmacol Sci*. 2010;31(4):161–74.

40. Korb O, Stützle T, Exner TE. Empirical scoring functions for advanced protein-ligand docking with PLANTS. *J Chem Inf Model*. 2009;49(1):84–96.

41. Mooij WT, Verdonk ML. General and targeted statistical potentials for protein-ligand interactions. *Proteins*. 2005;61(2):272–87.

42. Yasmin F, Nazli Z-i-H, Shafiq N, Aslam M, Bin Jardan YA, Nafidi H-A, Bourhia M. Plant-based bioactive phthalates derived from *Hibiscus rosa-sinensis*: As in vitro and in silico enzyme inhibition. *ACS Omega*. 2023;8(36):32677–89. https://doi.org/10.1021/acsomega.3c03342

43. Omidpanah S, Saeidnia S, Saeedi M, Hadjiakhondi A, Manayi A. Phthalate contamination of some plants and herbal products. *Bol Latinoam Caribe Plant Med Aromat*. 2018;17(1):61–7.

Supplementary Files

This is a list of supplementary files associated with this preprint. Click to download.

- InVitroandInSilicoEvaluationoftheEfficacyandSafetyofaGhanaianHerbalMedicinefortheTreatmentofOnchocerciasisandAfricanTrypanosomiasisSupplemer